Eur. Phys. J. B **21**, 67–73 (2001)

THE EUROPEAN PHYSICAL JOURNAL B
EDP Sciences

Magneto-optical Faraday and Kerr effect of orthoferrite thin films at high temperatures

N. Keller[1,a], J. Mistrík[1,2], Š. Višňovský[2], D.S. Schmool[3], Y. Dumont[4], P. Renaudin[1], M. Guyot[1], and R. Krishnan[1]

[1] Laboratoire de Magnétisme et d'Optique, Université de Versailles - CNRS, bâtiment Fermat, 45 avenue des États-Unis, 78035 Versailles Cedex, France
[2] Institute of Physics, Charles University, Ke Karlov 5, 121 16 Prague 2, Czech Republic
[3] Departamento de Física, Faculdade de Ciências, Universidade do Porto, Rua Campo Alegre 687, 4169 007 Porto, Portugal
[4] Département de Physique, Université de Versailles, 45 avenue des États-Unis, 78035 Versailles Cedex, France

Received 28 July 2000

Abstract. Orthoferrites present, as bulk materials, reorientation transitions of their magnetic moment alignment at temperatures depending on the rare-earth (RE) ion. In particular, orthoferrites ($\mathrm{REFeO_3}$) with RE = Sm, Dy, present this transition at $T_{\mathrm{SRT}} = 443$ K and 36 K, respectively. The spectra of the complex Kerr and Faraday angle have been measured on orthoferrite thin films (RE = Sm, Dy, Y), which were prepared by pulsed laser deposition on amorphous quartz substrates. The obtained spectra exhibit contributions of both surfaces and interfaces. Propagation effects of the polarized light in the magneto-optical medium which is interpreted in terms of a simplified theoretical formalism, is also observed. For selected photon energies, temperature dependent Faraday rotation measurements, Θ_{F}, on orthoferrite thin films (RE = Sm, Dy, Y) have been performed. A quite different thermal variation compared to the bulk magnetization has been observed. Curie temperatures are found to be close to the bulk values or slightly larger by 10 K to 20 K as in the case of $\mathrm{DyFeO_3}$ and $\mathrm{YFeO_3}$. For RE = Sm and Dy, Θ_{F} increases with increasing temperature contrary to the saturation magnetization, passes through a maximum at about 460 K and vanishes with a T_{C} of 647 ± 18 K, 695 K for RE = Sm and Dy respectively.

PACS. 75.50.Gg Ferrimagnetics – 75.70.Ak Magnetic properties of monolayers and thin films – 78.20.Ls Magnetooptical effects

1 Introduction

The study of the magnetic and magnetic-optical properties of magnetic oxide thin films has gained interest since the application of a new preparation technique, pulsed laser deposition (PLD), to the growth of perovskite thin films [1]. It can be expected that properties like the anisotropy and the magnetic exchange will strongly depend on the dimensionality of the films. The magnetic and magneto-optical properties of polycrystalline and single crystalline orthoferrites have already been studied intensively [2,3]. However, to date, very little is known about their properties in low dimensional films.

Former research concentrated on the interesting anisotropic optical and magnetic properties of these rare earth iron perovskites. The $\mathrm{REFeO_3}$ exhibits a very small ferromagnetic moment which originates from a partially compensated antiferromagnetic alignment of the magnetic moments situated on the Fe-sites. Particularly interesting are the $\mathrm{REFeO_3}$ systems as they also present reorientation transitions for their spin arrangement which depend on the nature of the RE atom. Throughout this article we will concentrate on some selected $\mathrm{REFeO_3}$ systems with RE = Y, Sm, Dy and Gd. In general, three different kinds of magnetic spin configurations are encountered in the $\mathrm{REFeO_3}$ (see Refs. [3–5]), $\Gamma_1(0)$, $\Gamma_2(F_a)$ and $\Gamma_4(F_c)$. They all involve a canted antiferromagnetic (AF) ordering of the moments on the iron sublattices [4] in the orthorhombic unit cell [6]. The $\Gamma_1(0)$ configuration designates an AF alignment of the spins along the *b*-axis in the *ab*-plane with a small canting along the *c*-axis and a zero resulting ferromagnetic moment. The $\Gamma_2(F_a)$ configuration describes an AF alignment of the spins along the *c*-axis in the *bc*-plane with a canting along the *a*-direction, whereas $\Gamma_4(F_c)$ describes an alignment of the spins along the *a*-axis in the *ab*-plane with a canting along the *c*-direction. The canting of the spins results in a small net ferromagnetic moment. Just below the Curie temperature (T_{C}) all considered $\mathrm{REFeO_3}$ present the $\Gamma_4(F_c)$ configuration. Upon decreasing the temperature, $\mathrm{SmFeO_3}$ and $\mathrm{DyFeO_3}$ pass through a spin reorientation transition (SRT) at 443 K and 36 K respectively. Below the respective temperatures where the SRT occurs, $\mathrm{SmFeO_3}$ assumes a $\Gamma_2(F_a)$ spin configuration *via* a continuous rotation of the magnetic moments [7] and $\mathrm{DyFeO_3}$ realizes a $\Gamma_1(0)$ configuration [8].

---

[a] e-mail: `keller@physique.uvsq.fr`

Table 1. Characteristic values of the electronic configuration, the ionic radius of the RE^{3+} in sixfold coordination, the canting angle, the Curie temperature, the temperature of the SRT and the assumed magnetic configuration for some $REFeO_3$.

RE	electronic configuration	ionic radius (RE^{3+}) (Å)	α (mrad)	T_C (K)	T_{SRT} (K)	Γ
Gd	$4f^7 5d^1 6s^2$	1.078	9.8	663	-	$\Gamma_4(F_z)^a$
Y	$4d^1 5s^2$	1.040	8.9	643	-	$\Gamma_4(F_z)$
Sm	$4f^6 5d^0 6s^2$	1.098	8.2	673	443 [7]	$\Gamma_4(F_z) \rightarrow \Gamma_2(F_x)$
Dy	$4f^{10} 5d^0 6s^2$	1.052	8.0	646	36 [8]	$\Gamma_4(F_z)^a \rightarrow \Gamma_1(0)$

[a] Iron and RE net moments are aligned parallel.

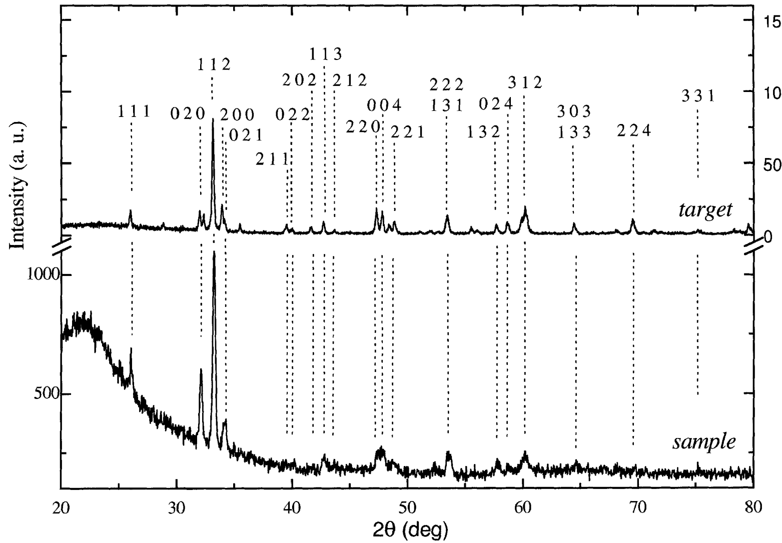

Fig. 1. X-ray diffraction pattern of a 1200 Å thick single phase $YFeO_3$ film. Also shown is the indexation of the $YFeO_3$ Bragg reflections and their relative intensities.

In the high temperature region, $T > 300$ K, all of the $REFeO_3$ exhibit a similar temperature dependence of the saturation magnetization. *A priori*, the Curie temperature varies depending on the nature of the RE ion (*cf.* Tab. 1).

Also $SmFeO_3$ does not exhibit a discontinuous behavior of its saturation magnetization at the SRT.

Magneto-optical Faraday rotation measurements have been performed up to now on thin single crystalline platelets of orthoferrites (*e.g.* Ref. [9]). Recently we reported on the crystal growth, the magnetic and magneto-optical properties of polycrystalline thin orthoferrite films grown by pulsed laser deposition [10,11]. In particular, the magneto-optical properties of $REFeO_3$, with RE = Gd, Y, Sm and Dy, have been studied in a limited temperature range from 300 to 550 K. The Faraday rotation (θ_F) decreased with increasing temperature only for $GdFeO_3$ and $YFeO_3$, whereas, surprisingly, θ_F increased with increasing temperature for the other compounds, $SmFeO_3$ and $DyFeO_3$, before passing through a maximum at about 450 K. As both $SmFeO_3$ and $DyFeO_3$ exhibit a similar thermal variation of θ_F and as only $SmFeO_3$ presents a SRT at 440 K, it seems unlikely that this increase is linked to the SRT. However, the main differences between the four orthoferrite systems resides in their electronic configuration. Both $GdFeO_3$ and $YFeO_3$ have unpaired $5d$ or $4d$ electrons, whereas both $SmFeO_3$ and $DyFeO_3$ have completed $4d$ shells. As the magneto-optical effects are closely related to the allowed electron transitions in the energy level scheme, a difference in the magneto-optical response may be expected. In the remainder of this article, an extended study of the spectral dependence of the Kerr and the Faraday effect and the thermal variation of the Faraday rotation at selected photon energies, on a series of thin films will be presented.

2 Experimental details

A new series of $YFeO_3$ and $SmFeO_3$ thin films has been prepared by pulsed laser deposition (*cf.* [11]). The films were deposited on polished amorphous quartz substrates. A Nd:YAG laser was operated at a wavelength of 355 nm with an energy of 180 mJ/pulse and a repetition rate of 10 Hz. The laser beam was focused onto the target surface, resulting in an energy density of ~ 9 J/cm^2 and rastered across the target surface according to a square pattern in order to produce a homogeneous film deposition. The substrates were held at a temperature of 780 °C during deposition. An additional partial oxygen atmosphere of 95 mtorr was provided in order to assure the stoichiometric crystallisation of the deposited film.

Following these preparation conditions, an "*in situ*" growth of polycrystalline orthoferrite resulted. The films have been characterised by $\theta/2\theta$ X-ray diffraction scans and have been determined to be single phased. Figure 1 shows a typical diffraction pattern of a 1200 Å thick polycrystalline $YFeO_3$ film. All of the measured diffraction peaks can be indexed by the tabulated values of bulk $YFeO_3$, as can be seen from the "theoretical" lines also indicated in Figure 1. Moreover, from the relative intensities, it can be determined that the $YFeO_3$ film is slightly textured along the [020] direction. Similar results were obtained for the $SmFeO_3$ films.

In this study, only the polar Kerr and Faraday effect were measured. Two different experimental magneto-optical set-ups were used throughout this study. One is a magneto-optical spectrometer based on an azimuth modulation technique. Magneto-optical spectroscopy was performed in nearly normal incidence at photon energies ranging from 1.2 to 4.5 eV. The magnetic field in this set-up is applied normal to the surface of the thin films. In the second set-up, the magneto-optical Faraday rotation measurements were also performed using a polar configuration. The measurements are based, in this set-up, on a polarization modulation technique using an elasto-optical modulator and a lock-in amplifier. The spectral dependence of the Faraday rotation could be sampled by using a set of interferential filters ($\Delta\lambda \approx \pm 5$ nm) and a xenon lamp as a white light source. The thermal variation of the Faraday rotation was measured with a new custom designed vacuum oven, allowing a variation of the sample temperature from 290 to 840 K. The temperature control, *via* a standard PID regulator, allows a reproducibility and a stability of a chosen temperature better than ±1 K.

3 Results and discussion

For thin magnetic films on non-magnetic substrates, MO Kerr and Faraday spectra present reflection and transmission properties simultaneously, thus making a quantitative analysis more complicated. It has been shown [12,13], that the complex MO Kerr and Faraday angles can be easily analytically expressed when special conditions are considered, *e.g.* for an incident monochromatic wave of zero azimuth and ellipticity. In the particular case of a single magnetic layer on a transparent substrate, the complex Faraday (χ_t) and Kerr rotation (χ_r) angles can be expressed as follows:

$$\chi_t^{(0,2)} = \frac{\delta N_1}{2N_1(1 + r_{01}r_{12}\mathrm{e}^{-2\mathrm{i}\beta_1})} \times \left[\mathrm{i}(1 - \mathrm{e}^{-2\mathrm{i}\beta_1})(r_{01} - r_{12}) + 2\beta_1(1 - r_{01}r_{12}\mathrm{e}^{-2\mathrm{i}\beta_1})\right] \quad (1)$$

and

$$\chi_r^{(0,2)} = \frac{-\mathrm{i}(1 - r_{01}^2)\delta N_1}{2N_1(1 + r_{01}r_{12}\mathrm{e}^{-2\mathrm{i}\beta_1})(r_{01} + r_{12}\mathrm{e}^{-2\mathrm{i}\beta_1})} \times \left[(1 + r_{12}^2\mathrm{e}^{-2\mathrm{i}\beta_1})(1 - \mathrm{e}^{-2\mathrm{i}\beta_1}) + 4\mathrm{i}\beta_1 r_{12}\mathrm{e}^{-2\mathrm{i}\beta_1}\right] \quad (2)$$

with the Fresnel coefficients for a single interface having the form: $r_{n-1,n} = \frac{N_{n-1}-N_n}{N_{n-1}+N_n}$, the complex refractive index for circular right (+) and left (−) polarized light $(N_\pm)^2 = \epsilon_{xx} \pm \mathrm{i}\epsilon_{xy}$, $\delta N_1 = \frac{1}{2}(N_+ - N_-)$, $\beta_1 = N_1\frac{\omega}{c}t_1$ and t_1 as the thickness of the film. Regrouping the terms of the formulas (1) and (2) more schematically, one can identify a term related to the interface/surface effects and one to the propagation of light.

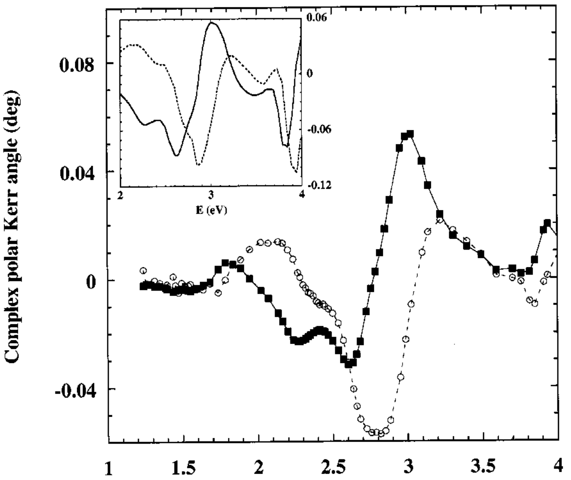

Fig. 2. Kerr rotation (solid squares) and ellipticity (open dots) measured on a $t_1 \sim 800$ Å thick $SmFeO_3$ film. The inset shows a model calculation for a 52 nm thick $SmFeO_3$ layer for the Kerr rotation (solid line) and the ellipticity (dashed line).

$$\chi_t^{(0,2)} = f_1\mathrm{i}\delta N_1(1 - \mathrm{e}^{-2\mathrm{i}\beta_1}) + f_2\frac{\omega}{c}\delta N_1 t_1 \quad (3)$$

and

$$\chi_r^{(0,2)} = f_3\mathrm{i}\delta N_1(1 - \mathrm{e}^{-2\mathrm{i}\beta_1}) + 4f_4\frac{\omega}{c}\delta N_1 t_1\mathrm{e}^{-2\mathrm{i}\beta_1} \quad (4)$$

where f_1, f_2, f_3 and f_4 depend only on the refractive indices. In the limit of ultrathin films, where $\mathrm{e}^{-2\mathrm{i}\beta_1} \approx 1$, both χ_r and χ_t are directly proportional to the thickness of the film: $\chi_{r,t} \propto \frac{\omega}{c}\delta N_1 t_1$. In the opposite extreme of very thick films, the usual dependence of the Kerr rotation on the dielectric tensor elements is recovered as $\exp(-2\mathrm{i}\frac{\omega}{c}N_1 t_1) \propto \exp(-2\frac{\omega}{c}N_1'' t_1) \to 0$ for $t \gg 1$. In the thickness range of moderately thick films, a combination of both the propagation and interface terms are important for the complex Kerr angle, which may even exhibit some oscillatory behaviour as a function of the film thickness ($\propto \exp(-2\mathrm{i}\frac{\omega}{c}N_1 t_1)$). It may be expected, in these circumstances, that the Faraday rotation should exhibit a more detailed fine structure in the energy spectrum than the Kerr rotation.

In Figures 2 and 3 we present the complex Kerr and Faraday angle measurements performed on a thin polycrystalline film of $SmFeO_3$ with a thickness of 800 ± 50 Å. Both the Kerr rotation and ellipticity show a structured spectrum as a function of the photon energy. As has been investigated previously (Ref. [5] and references therein), a multitude of electronic transitions are present in the energy range of 2 to about 5 eV due to charge transfer (CT) and CT-enhanced crystal electric field transitions (CT-CEF) of the octahedrally coordinated Fe^{3+} ions which are

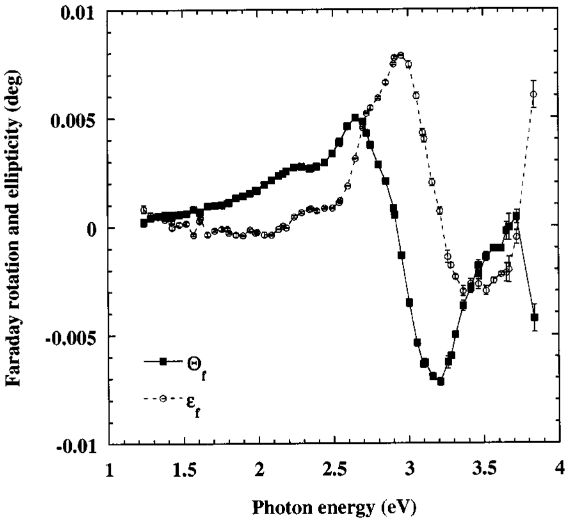

Fig. 3. Faraday rotation (solid squares) and ellipticity (open dots) measured on a $t_1 \sim 800$ Å thick SmFeO$_3$ film.

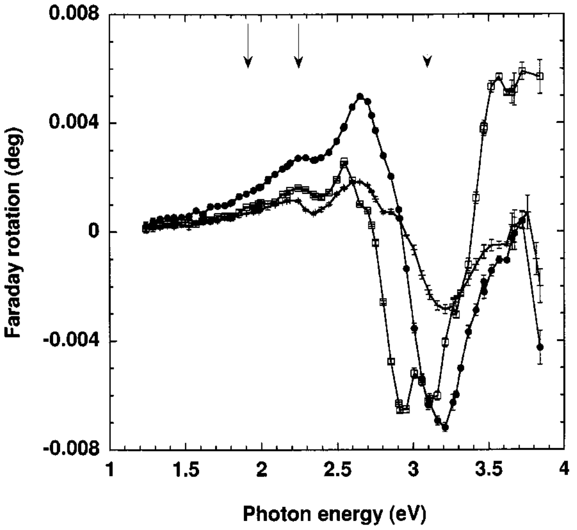

Fig. 4. Faraday rotation measured on SmFeO$_3$ (dots), YFeO$_3$ (squares) and GdFeO$_3$ (crosses) films. The arrows mark the photon energies used for the high temperature Faraday rotation measurements.

surrounded by six O^{2-} ions. According to Kahn *et al.* [5], at least seven transitions should be identified in the photon energy range of 1.2 to 4 eV investigated in the present study. Three should be CT transitions at 3.0, 3.15 and 3.85 eV, representing $t_{2u}^{n}(\pi) \rightarrow t_{2g}^{*}$, $t_{1u}^{n}(\pi) \rightarrow t_{2g}^{*}$ and $t_{1u}(\sigma) \rightarrow t_{2g}^{*}$ transitions respectively. The remaining four transitions should be of a CT-CEF type, at energies of 2.35, 2.68, 3.10 and 3.6 eV, representing ${}^6A_{1g} \rightarrow {}^4E_g({}^4G)$, ${}^6A_{1g} \rightarrow {}^4T_{2g}$, ${}^6A_{1g} \rightarrow {}^4E_g({}^4P)$ and ${}^6A_{1g} \rightarrow {}^4T_{1g}$ electronic excitations, respectively. All these transitions can be identified in the measured Kerr angle spectrum. However, the transition energies seemed to be shifted towards lower energies below 3 eV. Also a direct comparison of the Kerr rotation and ellipticity of Figure 2 to the corresponding data obtained by Kahn *et al.* [5] on single crystals, shows that the ellipticity measured on the films corresponds more closely to the rotation measured on the single crystal. The corresponding statement holds for the measured Kerr rotation on the film. This at first intriguing finding is closely related to the phenomenon of light propagation in thin films as explained by equation (2). The data in Figure 2 clearly shows that reflection and propagation effects are being mixed, as explained above. Once the dielectric tensor elements are known, it is possible to calculate the complex Kerr spectra by applying formula (2). The index of refraction, n, and the absorption coefficient, k, have been determined for a thick polycrystalline SmFeO$_3$ film by spectroscopic ellipsometry. Using the off-diagonal tensor elements determined by Kahn *et al.* [5], it is possible to calculate the theoretical Kerr spectrum for different thicknesses of an ideal SmFeO$_3$ layer. The inset in Figure 2 shows the result of these calculations for a 52 nm thin film, which reproduces best the experimental Kerr spectrum. Qualitatively, the agreement between the experiment and the simulation is rather satisfying. However, one may remark the slight difference in amplitudes, which can be explained by the fact that the available applied magnetic field was insufficient to saturate entirely the magnetisation (see Ref. [11]).

As the complex Faraday rotation is predominantly dependent on the propagation of the polarized light through the layer of thickness t_1 (see Eq. (1)), it would be more suitable to analyze the spectral features of the electronic transitions rather than the Kerr rotation. In Figure 3, the measured Faraday rotation and ellipticity on the same SmFeO$_3$ film are presented. All the different electronic transition energies can be identified by corresponding features in the spectrum. Also the dispersion relation seems to hold between the rotation and the ellipticity. Moreover, when considering only weak absorption ($k \ll n$), one can see from the general formulae that the Faraday rotation, $\chi_t = \theta_\mathrm{F} + \mathrm{i}\epsilon_\mathrm{F} \approx \left(\frac{\omega}{2cN_1}t_1\right)\delta N_1$, is directly proportional to the Kerr ellipticity, $\chi_r = \theta_\mathrm{K} + i\epsilon_\mathrm{K} \approx \left(\frac{1}{N_1(N_1^2-1)}\right)\mathrm{i}\delta N_1$ [14]. Comparing the measured Faraday rotation of the SmFeO$_3$ film to the Kerr ellipticity, as determined by Kahn *et al.* [5], one sees that this relation holds for photon energies of less than ~ 4 eV. From equations (1) and (2) we should expect the Faraday rotation to present more spectral features than the Kerr rotation. However analyzing the Faraday rotations (Fig. 4) and ellipticities (Fig. 5) measured on three different REFeO$_3$ films (RE = Sm, Y, Gd), one realizes that the spectral variations of both the Faraday rotation and the ellipticity, for photon energies smaller than ~ 2.5 eV, are washed out compared to the dielectric tensor elements determined on bulk single crystals (*cf.* [5]). This may be explained in one of two ways. The first one is related to the penetration depth of the light in the deposited layer. For photon energies up to 2.5 eV, the penetration depth of the light corresponds approximately to or is larger than the thickness of the orthoferrite layer. As a result, surface and interface effects make a significant contribution to the complex

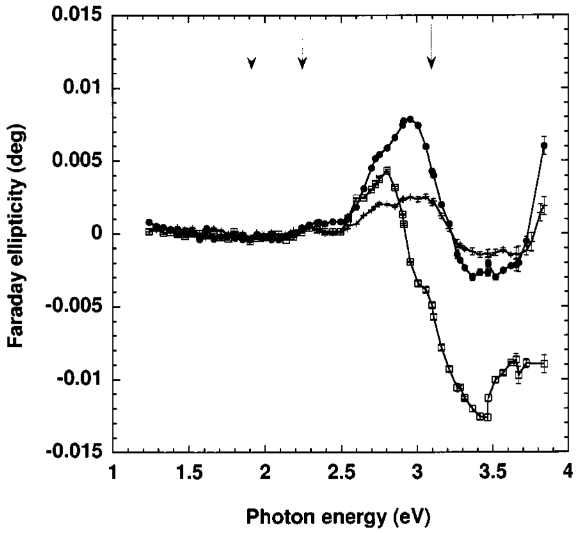

Fig. 5. Faraday ellipticity measured on $SmFeO_3$ (dots), $YFeO_3$ (squares) and $GdFeO_3$ (crosses) films. The arrows mark the photon energies used for the high temperature Faraday rotation measurements.

Faraday angle. Roughness at the surface has a particularly important influence by smoothing the features of the spectrum. The mean roughness as determined by AFM measurements on 13 μm × 13 μm square areas, shows typical values of 35 nm. The second possibility is related to the optical properties of orthoferrites. $REFeO_3$ are intrinsically birefringent. It was mentioned earlier that the obtained films show a weak preferential growth direction along the [020] direction (see Fig. 1). Hence, the films are not entirely polycrystalline with a random distribution of the crystallites throughout the film. A TEM study has shown that the crystallites have typical sizes of $\sim$ 100 nm. In the presence of a birefringent medium, it can be shown that the Faraday rotation is no longer a linear increasing function of the film thickness, but may exhibit an oscillating behaviour due to the presence of birefringence and due to the difference in the dielectric tensor components for the optical axis. The presence of these birefringent crystallites will result in an enlargement of the spectral transition lines (*i.e.* a broadening of this spectral feature).

Though the details in the rotation and ellipticity spectra are slightly different for the three different orthoferrite films ($SmFeO_3$, $YFeO_3$ and $GdFeO_3$) in Figures 4 and 5, the different CT and CT-CEF electronic transitions can still be identified and the overall photon energy dependences of the spectra are very similar.

We would like to emphasize here that the obtained $REFeO_3$ thin films seem to be single phased from the crystallographic as well as from the spectroscopic analysis.

For selected films of $REFeO_3$, with RE = Sm, Dy and Y, high temperature Faraday rotation measurements have been performed in order to assess the Curie temperatures of the films and to study whether the SRT of $SmFeO_3$ can be studied by means of MO measurements. Figures 6, 7 and 8 present the results obtained on $SmFeO_3$, $DyFeO_3$ and $YFeO_3$ films, respectively.

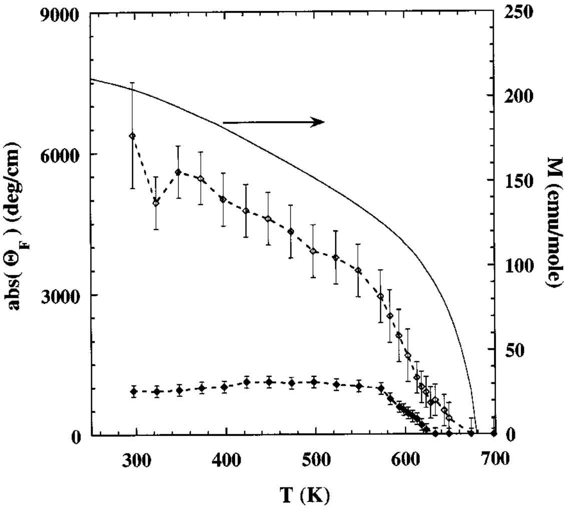

Fig. 6. Thermal dependence of the Faraday rotation measured on a $SmFeO_3$ film (t_l = 4280 ± 380 Å) for photon energies of 3.10 ± 0.04 eV (open diamonds) and 2.25 ± 0.02 eV (filled diamonds). The value of θ_F measured at 3.10 eV has been multiplied by a factor of -1 for convince of presentation (*cf.* Fig. 4 for sign of θ_F). The absolute value of the rotation is presented and compared to the temperature dependence of the bulk magnetization (line).

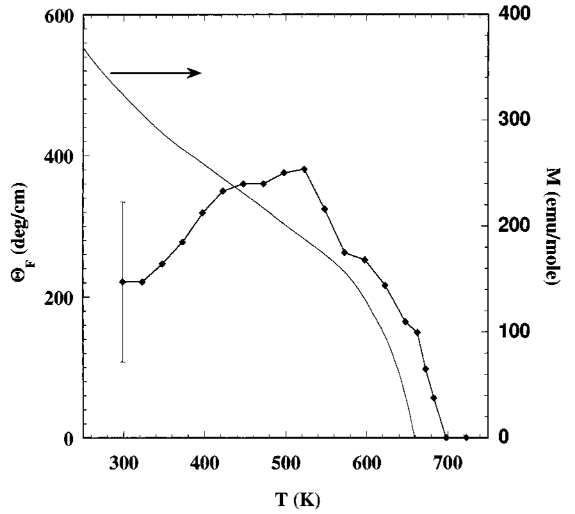

Fig. 7. Thermal dependence of the Faraday rotation measured on a $DyFeO_3$ film (t_l = 3240 ± 200 Å) for a photon energy 2.25 ± 0.02 eV (filled diamonds). The rotation is compared to the temperature dependence of the bulk magnetization (line).

The measurements performed on a 4280 ± 380 Å thick $SmFeO_3$ film were realised at two different photon energies, 2.25 ± 0.02 eV and 3.10 ± 0.04 eV, see Figure 6. In this figure the sign of θ_F is neglected for the ease of presentation (*cf.* Fig. 4 for the sign of θ_F at different photon energies). At 2.25 eV the previously observed broad maximum of θ_F at around 475 K (*cf.* [11]) can still be observed, whereas at 3.10 eV a more regular thermal variation compared to the bulk magnetization (solid line) can be observed. The Curie temperatures (T_C) observed for the two

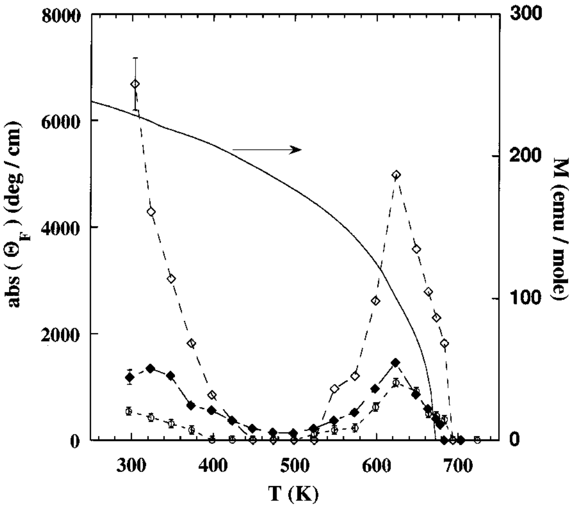

Fig. 8. Thermal dependence of the Faraday rotation measured on a $YFeO_3$ film (t_1 = 2420 ± 240 Å) for photon energies of 3.10 ± 0.04 eV (open diamonds), 2.25 ± 0.02 eV (filled diamonds) and 1.91 ± 0.02 eV (dots). The value of θ_F measured at 3.10 eV has been multiplied by a factor of −1 for convenience of presentation (*cf.* Fig. 4 for sign of θ_F). The absolute value of the rotation is presented and compared to the temperature dependence of the bulk magnetization (line).

photon energies vary slightly from each other and are both inferior to the bulk T_C of 673.6 K [7]. Experimentally, a T_C of 647.0 ± 18.0 K is determined. A precise determination of T_C at a photon energy of 2.25 eV was very difficult due to the resolution of the magneto-optical set-up. Also the relative errors become significant for increasing photon energy as the signal-to-noise ratio diminishes due to the onset of the optical absorption. As regards the SRT which occurs in $SmFeO_3$ at $T_{SRT} \approx 443$ K, no anomaly could be detected in the θ_F results for measurements at the two different photon energies.

The second orthoferrite studied, was a $DyFeO_3$ thin film with a thickness t_1 = 3240 ± 200 Å. The thermal variation of the θ_F as measured at a photon energy of 2.25 ± 0.02 eV is shown in Figure 7. At this photon energy θ_F nearly vanishes and combined with the non negligeable uncertainty of the film thickness the error on the measured rotation becomes important. As in our previous study [11] an initial increase with increasing temperature is observed. The Faraday rotation passes through a maximum before disappearing at a T_C of 695 K which compares to a bulk Curie temperature of $T_{C,bulk}$ = 646.6 ± 2.5 K. It is well known that $DyFeO_3$ presents a SRT at 35 K [8], therefore the maximum in the θ_F at about 500 K has probably a different origin.

The third $REFeO_3$ system, which we studied most intensively, is $YFeO_3$. Thin films of varying thicknesses, 1494, 2370, 2420 and 4280 Å, have been prepared and studied. In Figure 8 we present only characteristic data measured on a 2420 Å thick film at three photon energies, 1.91 ± 0.02 eV, 2.25 ± 0.02 eV and 3.10 ± 0.04 eV. Again, in this figure the sign of θ_F is neglected for the ease of presentation (*cf.* Fig. 4 for the sign of θ_F at different photon energies). The increase in the error bars with increasing photon energy is related to the diminishing signal-to-noise ratio at the onset of the optical absorption. The previously observed rapid decrease of θ_F with increasing temperature [11] can be confirmed. However, for temperatures above 500 K θ_F exhibits a significant increase and passes through a maximum at ∼ 620 K. The average Curie temperature determined from these measurements is 689.3 ± 4.0 K which is slightly more elevated than the bulk T_C of 642.6 ± 2.5 K. Also presented in Figure 8 is the thermal variation of the saturation magnetization (solid line) as measured on bulk samples.

In the light of this surprising thermal variation of θ_F further details of the experiment need to be considered. First, one might be tempted to postulate the presence of a compensation point due to two different phases in the samples. However, from the structural analysis (*cf.* Fig. 1) no second phase could be detected. The presence of a compensation point would imply that the sign of the hysteresis loop should change when increasing the temperature from ambient temperature towards T_C. But, the sign of the measured hysteresis loops remains the same throughout the entire temperature range. Therefore, we discard the possibility of a compensation of two MO contributions. The orthoferrites themselves do not have two different magnetic sublattices, but one lattice of canted antiferromagnetically coupled spins. Therefore, they do not provide an intrinsic means of a compensation phenomenon as in rare-earth iron garnets.

It was not yet stated in this article, but the hysteresis loops observed on the orthoferrite thin films present an extremely large coercive field of typically 1.4 to 1.8 T (see [11]). This implies that, for the Faraday rotation measurements we present here, the data was taken from minor hysteresis loops, as our experimental set-up did not allow to apply magnetic fields larger than 1.4 tesla. One may argue now, that this cancellation of θ_F at $T \sim 450$ K is purely an effect of the unsaturated hysteresis loops. Therefore, we tried to convince ourselves of the relevance of this result by performing a different experiment. Cooling a ferromagnetic sample from above its Curie temperature in an external static applied magnetic field is usually sufficient to saturate the magnetization along the field direction. Then it can be assumed that the relative thermal variation of the magnetization reflects the saturated state. This kind of experiment, a measurement of the relative change in the Faraday rotation of the 2420 Å thick $YFeO_3$ film upon cooling through the Curie temperature, was performed. The measured θ_F exhibits a similar thermal variation as presented in Figure 8. Therefore, we do not think that this phenomenon is related to the unsaturated state in which our measurements were made.

Up to this point, we have not considered the possible influence of the temperature on the electronic excitation spectra of the dielectric tensor elements. Indicated in Figures 4 and 5 (arrows) are the photon energies used for the present study of the thermal variation of the Faraday rotation. It is not unlikely that the positions of the electronic transition lines in the energy spectrum, as well as their width, vary with increasing temperature, hence modifying the observed Faraday rotation significantly. On a closer inspection of Figures 4 and 5, one sees that data on the Faraday rotation taken at energies of 2.25 eV and 3.10 eV may be subjected to this kind of influence. Therefore, we conclude that changes in the energy spectra of the dielectric tensor elements may cause the initial increase of θ_F observed in $SmFeO_3$, $DyFeO_3$ (*cf.* Figs. 6 and 7). This increase of θ_F is balanced at a higher temperature by the thermal reduction of the magnetization, which dominates θ_F close to T_C. A somewhat different situation arises for photon energies below 2 eV. In a generic way, a MO spectrum of magnetic oxides can be separated into two parts: a first one related to the electronic excitation of CT and CT-CEF nature in the visible and ultra-violet spectral range and a second one mainly related to the 'magnetic' excitation in the red and near infrared spectral range. Whereas purely electronic excitations are probed by photon energies of 2.25 and 3.10 eV, this situation is not so clear for the photon energy of 1.91 eV. The spectra of the Faraday rotation (Fig. 4) and the ellipticity (Fig. 5) do not show pronounced variation in the vicinity of 1.91 eV. Therefore, at least part of the cancellation of the Faraday rotation of the $YFeO_3$ thin film may have a different origin than a displacement or broadening of the spectrum with an increase in temperature (*e.g.* the occurrence of a phase transition of structural and/or magnetic origin).

4 Conclusion

New results on the temperature dependence of the magneto-optical properties of $REFeO_3$ thin film produced by pulsed laser ablation have been presented. The obtained films are single phase slightly textured polycrystalline, where all the diffraction peaks of bulk $REFeO_3$ could be identified in the X-ray diffraction pattern. Magneto-optical Kerr and Faraday spectroscopies have been performed on $REFeO_3$ films, with RE = Sm, Y and Gd. The obtained spectra could be explained with the help of a model describing the light propagation and the change of polarisation through a thin magnetic layer on a transparent substrate. Compared to reference data obtained by Kahn *et al.* [5], it can be stated that the obtained films present the same energy excitations as the referenced single crystals. The Curie temperatures have been determined for $SmFeO_3$, $DyFeO_3$ and $YFeO_3$ thin films and values of 647, 695 and 689 K have been obtained respectively. These values vary from their respective bulk T_C of 673, 647 and 643 K by approximately less than 10%. A different thermal dependence of the Faraday rotation compared to the bulk saturation magnetization was observed for all three systems. For photon energies above 2 eV shifts in the excitation energies and changes in the transition width of the MO spectrum may be responsible for the observed phenomena in $DyFeO_3$ and $SmFeO_3$. For photon energies lower than ~ 2 eV the Faraday rotation and ellipticity are no longer influenced on a primary basis by the electronic charge transfer and crystal electric field transitions. Therefore, the cancellation of the Faraday rotation in the temperature range of 400 to 500 K in $YFeO_3$ may also have another source, for example the presence of a phase transition which can be structural and/or magnetic in nature. Further measurements and also purely magnetic studies are necessary to investigate the phenomenon more precisely.

We would like to thank A. Girard from ONERA in Paris for the first TEM measurements. The authors acknowledge the financial support in the form of a Barrande contract n°2000-010-1. D.S.S. acknowledges financial support from a Marie Curie research grant, number ERB4001GT971610, of the EU.

References

1. *e.g. Epitaxial Oxide Thin Films and Heterostructures*, Mater. Res. Soc. Symp. Proc., edited by D.K. Fork, J.M. Phillips, R. Ramesh, R.M. Wolf (Mater. Res. Soc., Warrendale, 1994), Vol. 341.
2. D. Treves, J. Appl. Phys. **36**, 1033 (1965).
3. R.L. White, J. Appl. Phys. **40**, 1061 (1969).
4. G.F. Hermann, Phys. Rev. **133**, A1334 (1964).
5. F.J. Kahn, P.J. Pershan, J.P. Remeika, Phys. Rev. **186**, 891 (1969).
6. S. Geller, E.A. Wood, Acta Cryst. **9**, 563 (1955).
7. E.M. Gyorgy, J.P. Remeika, F.B. Hagedorn, J. Appl. Phys. **39**, 1369 (1968).
8. G. Gorodetsky, B. Sharon, S. Shtrikman, J. Appl. Phys. **39**, 1371 (1968).
9. W.J. Tabor, A.W. Anderon, L.G. van Vitet, J. Appl. Phys. **41**, 3018 (1970).
10. R. Krishnan, A. Lisfi, M. Guyot, V. Cagan, J. Magn. Magn. Mat. **147**, L221 (1995).
11. D.S. Schmool, N. Keller, M. Guyot, R. Krishnan, M. Tessier, J. Appl. Phys. **86**, 5712 (1999).
12. R. Lopusnik, S. Visnovsky, N. Keller, M. Guyot, R. Krishnan, M. Tessier, J. Magn. Soc. Jpn **23**, 59 (1999).
13. S. Visnovsky, R. Lopusnik, M. Nyvlt, V. Prosser, J. Ferré, C. Train, P. Beauvillain, D. Renard, R. Krishnan, J.A.C. Bland, Czech. J. Phys. **50**, 857 (2000).
14. G.B. Scott, D.E. Lacklison, IEEE Trans. Magn. **4**, 292 (1976).